

Retraction

Retracted: Construction and Application of the Online Finance Credit Risk Rating Model Based on the Artificial Neural Network

Discrete Dynamics in Nature and Society

Received 10 October 2023; Accepted 10 October 2023; Published 11 October 2023

Copyright © 2023 Discrete Dynamics in Nature and Society. This is an open access article distributed under the Creative Commons Attribution License, which permits unrestricted use, distribution, and reproduction in any medium, provided the original work is properly cited.

This article has been retracted by Hindawi following an investigation undertaken by the publisher [1]. This investigation has uncovered evidence of one or more of the following indicators of systematic manipulation of the publication process:

- (1) Discrepancies in scope
- (2) Discrepancies in the description of the research reported
- (3) Discrepancies between the availability of data and the research described
- (4) Inappropriate citations
- (5) Incoherent, meaningless and/or irrelevant content included in the article
- (6) Peer-review manipulation

The presence of these indicators undermines our confidence in the integrity of the article's content and we cannot, therefore, vouch for its reliability. Please note that this notice is intended solely to alert readers that the content of this article is unreliable. We have not investigated whether authors were aware of or involved in the systematic manipulation of the publication process.

Wiley and Hindawi regrets that the usual quality checks did not identify these issues before publication and have since put additional measures in place to safeguard research integrity.

We wish to credit our own Research Integrity and Research Publishing teams and anonymous and named external researchers and research integrity experts for contributing to this investigation.

The corresponding author, as the representative of all authors, has been given the opportunity to register their agreement or disagreement to this retraction. We have kept a record of any response received.

References

- [1] Y. Mao, Z. Wang, X. Li, C. Li, and H. Wang, "Construction and Application of the Online Finance Credit Risk Rating Model Based on the Artificial Neural Network," *Discrete Dynamics in Nature and Society*, vol. 2021, Article ID 6926216, 11 pages, 2021.

Research Article

Construction and Application of the Online Finance Credit Risk Rating Model Based on the Artificial Neural Network

Yufeng Mao,^{1,2} Zongrun Wang,¹ Xing Li ,³ Chenggang Li,⁴ and Hanning Wang²

¹Business School, Central South University, Changsha 410083, China

²School of Big Data Application and Economics, Guizhou University of Finance and Economics, Guiyang 550025, China

³School of Management, Nanchang University, Nanchang 330031, China

⁴New Structure Finance Research Center, Guizhou University of Finance and Economics, Guiyang 550025, China

Correspondence should be addressed to Xing Li; xingli@mail.gufe.edu.cn

Received 17 August 2021; Revised 6 September 2021; Accepted 11 September 2021; Published 30 September 2021

Academic Editor: Ahmed Farouk

Copyright © 2021 Yufeng Mao et al. This is an open access article distributed under the Creative Commons Attribution License, which permits unrestricted use, distribution, and reproduction in any medium, provided the original work is properly cited.

The low-cost, highly efficient online finance credit provides underfunded individuals and small and medium enterprises (SMEs) with an indispensable credit channel. Most of the previous studies focus on the client crediting and screening of online finance. Few have studied the risk rating under a complete credit risk management system. This paper introduces the improved neural network technology to the credit risk rating of online finance. Firstly, the study period was divided into the early phase and late phase after the launch of an online finance credit product. In the early phase, there are few manually labeled samples and many unlabeled samples. Therefore, a cold start method was designed for the credit risk rating of online finance, and the similarity and abnormality of credit default were calculated. In the late phase, there are few unlabeled samples. Hence, the backpropagation neural network (BPNN) was improved for online finance credit risk rating. Our strategy was proved valid through experiments.

1. Introduction

Online finance is a low-cost, highly efficient means to provide services and attract consumers based on internet platforms, making the financial system in China much more inclusive. Online finance can operate in various modes, including online money management, online payment, and online consumer finance [1–5]. Among them, online finance credit provides underfunded individuals and small and medium enterprises (SMEs) with an indispensable credit channel [6–9]. To keep the risk within control, risk rating and control are necessary in the early and late phases after the launch of online finance credit products [10–14]. Therefore, the suitable rating of the online finance credit risk can effectively promote the performance of online finance enterprises in risk management, safe operation, and income generation.

Purohit and Kulkarni [15] constructed an evaluation system for the online finance credit risk control of SMEs, which covers four primary indices such as portfolio, quality,

cost, and robustness, and obtained the weight and score of each index through the analytic hierarchy process (AHP) and efficiency coefficient method (ECM). Kamboh et al. [16] put forward several countermeasures to the online finance credit risk: enhancing the organizational management of online finance enterprises, controlling the risk of credit businesses within a reasonable range, and optimizing the focus of the risk control department of online finance platforms.

Some scholars have analyzed the credit transformation of banks in the context of online finance development [17–21]. Considering the regulating effect of online finance, Xu et al. [22] evaluated the influence of green credit measures on bank performance, constructed an evolutionary game model for the online finance enterprise and loan enterprise, and verified that online finance can effectively weaken the influence of green credit on bank performance. Fayyaz et al. [23] conducted big data analysis on the financial data before, during, and after online finance credit products are issued to SMEs, summarized the big data warning

conditions (including risk process and internal evaluation application system, banking operation system, data warehouse platform, risk data market, capital metering, and decision support system), and constructed a risk management and warning system based on the analysis results.

Most of the previous studies focus on the client crediting and screening of online finance. Few have studied the risk rating under a complete credit risk management system [24–28]. Capable of solving most nonlinear mapping problems, backpropagation neural network (BPNN) can correctly mine the deep relationships between the indices and values of online finance credit risks. By virtue of the superiority of the artificial neural network in nonlinear mapping, this paper introduces the BPNN to the risk rating of online finance credit products. The main contents of this research are as follows: after the launch of an online finance credit product, there are few manually labeled samples and many unlabeled samples in the early phase. To adapt to this situation, Section 2 designs a cold start method for the credit risk rating of online finance and calculates the similarity and abnormality of the credit default. In the late phase, there are few unlabeled samples. Hence, Section 3 improves the wolf pack algorithm (WPA) based on the belief learning model and relies on the improved WPA to optimize the BPNN. The improved BPNN was adopted to rate the online finance credit risk, which effectively avoids the subjectivity in weight assignment. The proposed model was proved effective through experiments.

2. Cold Start of the Risk Rating Model in the Early Phase

Online finance credit risk rating is a key step in the risk control of online finance credit. Traditional online finance credit risk rating models need to be constructed based on enough historical labeled samples. If there are not enough such samples, the modeling personnel of the early-phase risk rating model must fully understand the risk control rules of the credit product. New methods are necessary to realize the cold start of the online finance credit risk model.

After the launch of an online finance credit product, there are few manually labeled samples and many unlabeled samples in the early phase. To adapt to this situation, this paper designs a cold start method for online finance credit risk rating. By machine learning, the proposed method can obtain useful samples out of many unlabeled samples and provide sufficient data for subsequent training of the online finance credit risk rating model based on the neural network.

Let $a = S\xi$ be the sample space of online finance credit risk rating; $B = \{-1, 0, +1\}$ be the label space; and b be the indicator of sample labeling. If $b = +1$, the corresponding sample is labeled “client default,” i.e., payment is not completed on time; if $b = 0$, the sample is labeled “normal,” i.e., payment is completed on time; if $b = -1$, the sample is not labeled.

Suppose there exists a dataset of n samples $TS = \{(a_1, b_1), \dots, (a_k, b_k), \dots, (a_n, b_n)\}$, where $a_i \in A$ is a sample in the dataset. The first k samples of the dataset are labeled: $TS^k = \{(a_{k+1}, b_{k+1}), \dots, (a_n, b_n), \dots, (a_n, b_n)\}$. The remaining $n - k$ samples are labeled: $TS^v = \{(a_{k+1}, b_{k+1}), \dots, (a_n, b_n), \dots, (a_n, b_n)\}$. For TS^v , the potential default samples and normal samples were determined based on the calculated similarity and abnormality of the credit default.

2.1. Default Similarity. Suppose dataset $TS = \{a_i\}_i^m$, which is equal to 1, possesses two parameters: a hidden variable $C = (c_1, \dots, c_m)$ characterizing the cluster labels of samples and a class parameter $\Psi (\Psi_1, \dots, \Psi_l)$ of the model. Note that $c_m \in \{1, \dots, L\}$, and $C_i = l$ indicates that class i has l members. According to the Bayesian theory, the probability distribution satisfies $GV(\Psi, c|TS) \propto GV_0(\Psi)GV_0(c)GV(TS|\Psi, c)$.

The index data in this research are all multidimensional continuous variables obeying the multidimensional Gaussian random distribution. Let Ψ be expectation λ . Then, $GV(a_i|\Psi, c) \sim M(v_{c_i}, \Theta)$. Conjugate prior $GV_0(\Psi_l) \sim M(0, \varepsilon^2 J)$ can be applied to $GV_0(\Psi)$. Let $m_l, l \in \{1, \dots, L\}$ be the number of data in class l . Then, the cluster prior $GV_0(c_l)$ of each sample can be generated by the Dirichlet process mixture model:

$$\begin{cases} GV(c_i = l|c_{-i}) = \frac{m_l}{m - 1 + \beta} \\ GV(c_i = L + 1|c_{-i}) = \frac{\beta}{m - 1 + \beta} \end{cases} \quad (1)$$

The first step is to randomly initialize parameters c and Ψ . Each c_i can be sampled by

$$GV(c_i = l|TS, \Psi, c_{-i}) \propto GV(c_i = l|c_{-i})GV(a_i|c, \Psi) = \frac{m_l}{m - 1 + \beta} \frac{1}{(2\pi)^{\xi/2} |\Theta|^{1/2}} e^{-(1/2)(a_i - \lambda_i)^T \sum^{-1} (a_i - \lambda_i)}. \quad (2)$$

The probability of establishing a new class $L + 1$ can be calculated by

$$\begin{aligned} GV(c_i = L + 1|TS, \Psi, c_{-i}) &\propto GV(c_i = L + 1|c_{-i})GV(a_i|c, \Psi) \\ &= GV(c_i = L + 1|c_{-i}) \int GV_0(\Psi_{L+1})GV(a_i|c_i, \Psi, \Psi_{L+1})\xi\Psi_{L+1} \\ &= \frac{\beta}{m - 1 + \beta} \frac{1}{(2\pi)^{\xi/2} \varepsilon^\xi} \frac{|\Theta'|^{1/2}}{|\Theta|^{1/2}} e^{-(1/2)a_i^T (\Theta^{-1}\Theta'\Theta^{-1} - \Theta^{-1})a_i} \\ &\text{where } \left(\Theta' = \left(\frac{1}{\varepsilon^2} I + \Theta^{-1} \right)^{-1} \right). \end{aligned} \quad (3)$$

When new data are added to class l , the parameter Ψ_l of that class should be updated by

$$\begin{aligned}
 GV(\Psi_l|TS, c) &\propto GV_0(\Psi_l) \prod_{i=1}^m GV(a_i|c, \Psi) \\
 &= GV_0(\Psi_l) \prod_{i_l=1} GV(a_i|c, \Psi) \\
 &\propto e^{-(1/2\varepsilon^2)\lambda_l^T \lambda_l - (1/2) \sum_{i_l=1} (a_i - \lambda_l)^T \sum^{-1} (a_i - \lambda_l)} \\
 &\sim M(\lambda_l', \Theta_l')
 \end{aligned}$$

where $\left(\lambda_l' = \Theta_l' \left(\sum_{i_l=1} a_i \right), \Theta_l' \left(\frac{1}{\varepsilon^2} J + \Theta^{-1} \right)^{-1}, d_l = \sum_{i=1}^m \gamma_{c,l} \right)$.

(4)

Let λ be the cluster mean. Then, the distance from sample a to a cluster can be measured by Euclidean distance:

$$\text{dist}(a, \lambda) = \sqrt{(a - \lambda)^T (a - \lambda)}. \quad (5)$$

If $a \in TS^v$, the minimum distance from a to the center of a cluster of normal samples, i.e., the similarity between a and a class of normal samples, can be calculated by

$$\text{DAL}(a) = \min_{i=1}^l \text{dist}(a, \lambda_i). \quad (6)$$

The similarity between a and a class of default samples can be calculated by

$$\text{DLT}(a) = \min_{i=1}^r \text{dist}(a, \lambda_i). \quad (7)$$

There are very few client default samples in the scenario of online finance credit risk rating. However, the model is expected to recognize potential default samples more accurately than normal samples. Comparing the results of formulas (6) and (7), the similarity $\text{SEM}(a)$ between a and a class of default samples can be modified as

$$\text{SEM}(a) = \frac{\text{DLT}(a)}{\text{DLT}(a) + \text{DAL}(a)}. \quad (8)$$

Formula (8) shows the following:

- (1) If $\text{DLT}(a) \gg \text{DAL}(a)$, $\text{SEM}(a)$ approximates 1, and the corresponding sample is a default sample
- (2) If $\text{DLT}(a) \approx \text{DAL}(a)$, $\text{SEM}(a)$ approximates 0.5, and the corresponding sample is not an obvious default sample
- (3) If $\text{DLT}(a) \ll \text{DAL}(a)$, $\text{SEM}(a)$ approximates 0, and the corresponding sample is a normal sample

2.2. Default Abnormality. All samples in the sample set were modeled by the isolation forest algorithm. Let $LT(XB(a))$ be the mean height of all isolation trees in the algorithm. Then, the default abnormality $\text{VEH}(a)$ of an unlabeled sample can be calculated by

$$\text{VEH}(a) = 2^{-LT(XB(a))}. \quad (9)$$

Formula (9) shows that the smaller $LT(XB(a))$, the greater $\text{VEH}(a)$ and the more likely for a sample to be a

potential default sample. If many unlabeled samples are not normalized, the $LT(XB(a))$ value will be relatively high. To prevent the problem, this paper adopts the mean path length of unsuccessful searches in the binary search tree for normalization. If there are M samples, then

$$d(M) = 2XB(M) - \left(2 \frac{(M-1)}{M} \right). \quad (10)$$

Let δ be the Euler–Mascheroni constant. Then, the number of harmonics $XB(M)$ in formula (10) can be estimated by

$$XB(M) = \ln(M) + \delta. \quad (11)$$

The normalized default abnormality $\text{VEH}(a)$ can be calculated by

$$\text{VEH}(a) = 2^{LT(XB(a))/d(M)}. \quad (12)$$

Formula (12) shows the following:

- (1) If $LT(r(a))$ approximates $d(m)$, $\text{VEH}(a)$ approaches 0.5, and the corresponding sample is not an obvious default sample
- (2) If $LT(r(a))$ approximates 0, $\text{VEH}(a)$ approaches 1, and the corresponding sample is a default sample
- (3) If $LT(r(a))$ approximates $m-1$, $\text{VEH}(a)$ approaches 0, and the corresponding sample is a normal sample

2.3. Sample Recognition and Weighting. $\text{SEM}(a)$ and $\text{VEH}(a)$ should be considered comprehensively to recognize potential default samples and normal samples from the unlabeled dataset. Let ω be the weight that balances the relative importance of $\text{SEM}(a)$ and $\text{VEH}(a)$. Then, the total score of online finance credit risk samples can be calculated by

$$RD(a) = \omega \text{VEH}(a) + (1 - \omega) \text{SEM}(a). \quad (13)$$

Let φ be the threshold for a sample to be a potential default sample. To judge a sample as a potential default sample, the total score must satisfy

$$RD(a) \geq \varphi. \quad (14)$$

Let α be the threshold for a sample to be a normal sample. To judge a sample as a normal sample, the total score must satisfy

$$RD(a) \leq \alpha. \quad (15)$$

The thresholds φ and α can be set in reference to the total risk rating scores for the potential default sample and normal sample in the labeled dataset. The mean φ of potential default samples $RD(a)$ can be calculated by

$$\varphi = \frac{1}{|TS_k^{+1}|} \sum_{i=1}^{|TS_k^{+1}|} RD(a_i). \quad (16)$$

The mean α of normal samples $RD(a)$ can be calculated by

$$\alpha = \frac{1}{|TS_k^{-1}|} \sum_{i=1}^{|TS_k^{-1}|} RD(a_i). \quad (17)$$

This paper sets the weight of each labeled sample to 1. For potential default samples, the higher the total score, the higher the confidence of its risk rating. The weight of these samples can be configured by

$$q(a) = \frac{RD(a)}{\max_a RD(a)}. \quad (18)$$

For normal samples, the higher the total score, the lower the confidence of its risk rating. The weight of these samples can be configured by

$$q(a) = \frac{\max_a RD(a) - RD(a)}{\max_a TS(a) - \min_a RD(a)}. \quad (19)$$

Finally, the loss function can be minimized by

$$\sum_i q_i k(b_i, g(a_i)) + \mu S(q). \quad (20)$$

3. Late-Phase Risk Rating Model

3.1. Model Construction. BPNN needs to be trained by sufficient samples. During the training, the error is back-propagated through the network and used to iteratively correct weights and thresholds. The regularity and information of the training data are memorized by the nodes in the network. During evaluation, the BPNN can output risk values once the indices are imported into the network. Since there are few unlabeled samples in the late phase after the launch of an online finance credit product, the BPNN was adopted to rate online finance credit risks, which effectively avoids the subjectivity in weight assignment. Figure 1 shows the topology of the BPNN.

Let Q and f be the connection weights and biases of the artificial neural network (ANN), respectively. Then, the input of hidden layer node j can be solved by

$$O = \sum_{i=1}^m q_{ji} \cdot a_i + f_j = q_j A + f_j. \quad (21)$$

The output of hidden layer node j can be calculated by the activation function g of the hidden layer:

$$b_j = g(O_j) = g\left(\sum_{i=1}^m q_{ji} \cdot a_i\right) = G(q_j A). \quad (22)$$

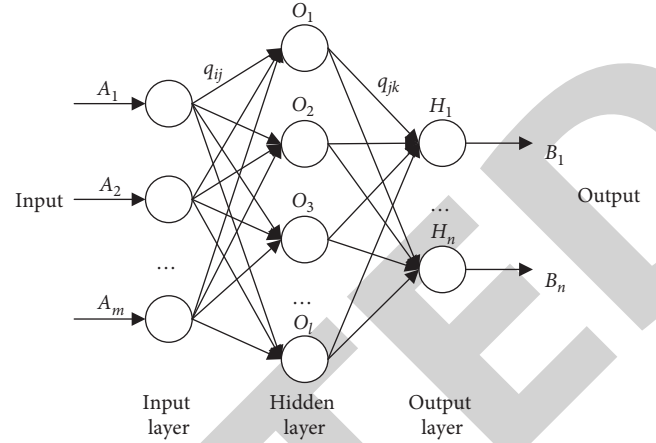


FIGURE 1: Topology of the BPNN.

The BPNN training can be trained in two stages: forward propagation and error backpropagation. The network training can be detailed as follows.

Based on the sample set of evaluation indices, the structure of input and output layers is determined for the neural network. To initialize the connection weights and biases, the activation function g of the hidden layer is generally a sigmoid function:

$$g(a) = \frac{1}{1 + e^{-a}}. \quad (23)$$

During the forward propagation of information, the output O_j of each hidden layer node can be calculated by

$$O_j = g\left(\sum_{i=1}^m q_{ij} a_i + f_j\right), \quad j = 1, 2, \dots, k. \quad (24)$$

The output b_l of each output layer node can be calculated by

$$b_l = \sum_{j=1}^k O_j q_{lj} + \varepsilon_l, \quad l = 1, 2, \dots, n. \quad (25)$$

The error σ_l of each output layer node can be calculated by

$$\sigma_l = B_l - P_l, \quad l = 1, 2, \dots, n. \quad (26)$$

Let ζ be the learning rate. During error backpropagation, the weights can be updated by

$$q_{ij}^* = q_{ij} + \zeta O_j (1 - O_j) a(i) \sum_{l=1}^n q_{jk} \sigma_k, \quad i = 1, 2, \dots, m; j = 1, 2, \dots, k; q_{jl}^* = q_{jl} + \zeta O_j \sigma_l, \quad j = 1, 2, \dots, k; l = 1, 2, \dots, n. \quad (27)$$

The bias can be updated by

$$f_j = f_j + \zeta O_j (1 - O_j) \sum_{l=1}^n q_{jl} \sigma_l, \quad j = 1, 2, \dots, k, \varepsilon_l = \varepsilon_l + \sigma_l, \quad l = 1, 2, \dots, n. \quad (28)$$

The training should be terminated when the error reaches the preset threshold or the number of iterations reaches the maximum.

3.2. Algorithm Optimization. The WPA is a stochastic probabilistic search algorithm, capable of finding the optimal solution at a high probability. Paralleled search is another feature of the algorithm: the search can start from multiple points at the same time to improve the algorithm efficiency; the points do not affect each other. The traditional BPNN converges slowly and easily falls into the local minimum. This paper improves the WPA based on the belief learning model and relies on the improved WPA to optimize the initial connection weights and biases of the BPNN. Figure 2 shows the process of the WPA.

Figure 3 explains the idea of neural network optimization with the WPA improved by the belief learning model. Firstly, a belief learning model was constructed for the virtual game between multiple individuals. Let N be the number of outside individuals and $D(d_1, d_2, \dots, d_i, \dots, d_l)$ be the set of strategies of these individuals. The belief weight for another outside individual j to choose strategy d_i can be calculated by

$$f_j^{\tau+1}(d_i) = \begin{cases} f_j^{\tau}(d_i) + 1, & \text{selected,} \\ f_j^{\tau}(d_i), & \text{not selected.} \end{cases} \quad (29)$$

Formula (31) shows that if the said outside individual j chooses strategy d_i in phase τ , then the belief weight should be increased by 1 in phase $\tau + 1$. The probability for individual j to choose strategy d_i obeys the following correlation with the belief weight of phase $\tau + 1$:

$$\lambda_j^{\tau+1}(d_i) = \frac{f_j^{\tau+1}(d_i)}{\sum_{i=1}^l f_j^{\tau+1}(d_i)}. \quad (30)$$

The expectation for inside individual j to choose strategy d_i can be derived from the cost $v_j^{\tau+1}(d_i/\lambda_j^{\tau+1} + 1(d_i))$ of an outside individual to choose a strategy:

$$v^{\tau+1}(d_i) = \sum_{j \in PE} v_j^{\tau+1} \left(\frac{d_i}{\lambda_j^{\tau+1}(d_i)} \right) \bullet \lambda_j^{\tau+1}(d_i). \quad (31)$$

In phase $\tau + 2$, the probability for an inside individual to choose strategy d_i can be calculated by

$$GV^{\tau+2}(d_i) = \frac{e^{v^{\tau+1}(d_i)}}{\sum_{i \in PE} e^{v^{\tau+1}(d_i)}}. \quad (32)$$

To optimize the response to future behaviors, every inside individual will choose the strategy with the maximum probability of the optimal response in phase $\tau + 2$.

The BPNN was optimized with the WPA improved based on the belief learning model in the following steps:

Step 1: initialize algorithm parameters, such as pack size, number of scout wolves, scout wolf movement factor, scout wolf movement distance factor, maximum number of iterations, and pack update ratio, and randomly initialize the pack. Complete the topology design of the BPNN.

Step 2: import the wolf positions and training samples into the neural network. Let N_T be the total number of weights and biases and $b_i - p_i$ be the output error of the i th node. Compute the absolute error between expectation and prediction by formula (33), and take it as the order concentration function for individual wolves in smelling prey:

$$WR = \sum_{i=1}^{N_T} |b_i - p_i|. \quad (33)$$

Select the head wolf, scout wolves, and ferocious wolves in turn based on the calculated concentrations.

Step 3: based on the results of the belief learning model, determine the most probable future wandering direction for scout wolves. Let B_i and B_{HW} be the distance of an individual wolf i and the head wolf to the prey, respectively. If B_i is greater than B_{HW} or the number of iterations surpasses the maximum number Φ_{\max} of wanderings, each individual wolf will compute its expectation for the next movement according to the historical wanderings of other individuals and determine the next wandering direction.

Step 4: compute the distance between individuals x and y by

$$ED(x, y) = \sum_{t=1}^{TS} |s_{xy} - s_{yt}| \bullet t_N = \frac{1}{TS \cdot \theta} \cdot \sum_{t=1}^{TS} |\max_y - \min_t|. \quad (34)$$

Let $[\text{Min}_t, \text{Max}_t]$ be the interval of the t th weight or bias to be optimized and γ_f be the step length of a ferocious wolf to approach the head wolf. Then, the ferocious wolf can approach the prey by

$$s_{it}^{l+1} = s_{it}^l + \gamma_f^t \cdot \frac{(h_t^l - s_{it}^l)}{|h_t^l - s_{it}^l|}. \quad (35)$$

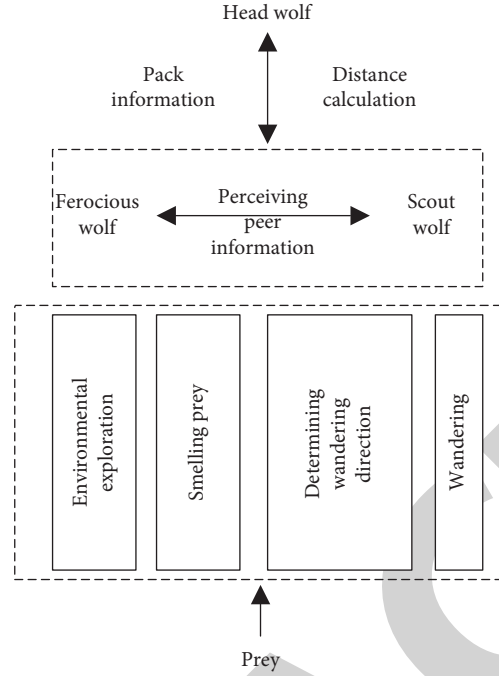


FIGURE 2: Process of the WPA.

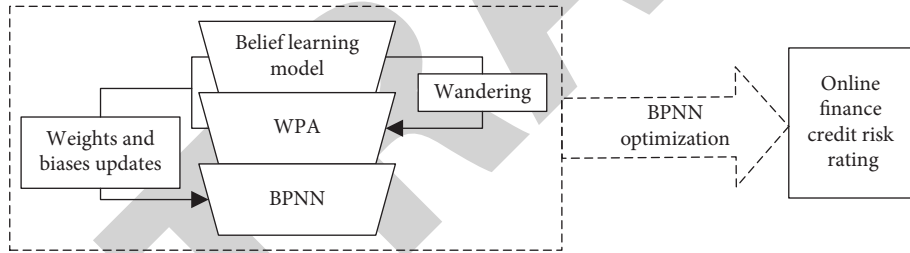


FIGURE 3: Idea of neural network optimization with the WPA improved by the belief learning model.

Formula (35) shows that if $B_i > B_{HW}$, then $B_{HW} = B_i$, and the ferocious wolf will replace the head wolf; if $B_i < B_{HW}$, then the ferocious wolf will continue to approach the prey until $t_l \leq t_N$.

Step 5: randomly choose a number Θ from $[-1, 1]$; define γ_d as the besieging step length of individual wolf i . Then, the state of each individual wolf during the besieging can be updated by

$$s_{it}^{l+1} = s_{it}^l + \Theta \cdot \gamma_d^t \cdot |H_t^l - s_{it}^l|. \quad (36)$$

Step 6: set the individual closest to the prey as the head wolf, and allocate the prey to the pack according to the contribution to foraging. Finally, remove the inferior individuals from the pack.

Step 7: after the end of iterations, import the head wolf position as the initial values of weights and biases into the neural network, and complete the network training.

Figure 4 illustrates the flow of the late-phase online finance credit risk rating model. The relevant parameters have been introduced in preceding parts.

4. Experiments and Results' Analysis

Receiver operating characteristic (ROC) is a curve drawn by a series of different dichotomy methods, with true positive (TP) as the ordinate and false positive (FP) as the abscissa. Unlike traditional evaluation metrics, ROC metric allows the existence of intermediate state, which reflects the actual situation, and applies to a wide range. By this metric, the test results can be divided into several sequential classes for statistical analysis. This paper adopts the AUC of the ROC curve to evaluate the performance of the online finance credit risk rating model. The number of labeled samples in the early phase after the launch of an online finance credit product was set to 20, and the proportion of potential default samples was adjusted from 0 to 0.5. Figure 5 shows the influence of that proportion on the AUC. With the growing proportion of potential default samples, the AUCs of STSSLA and our algorithm increased to a certain extent. Meanwhile, the AUC of isolation forest algorithm changed very little because the algorithm is an unsupervised method immune to labels.

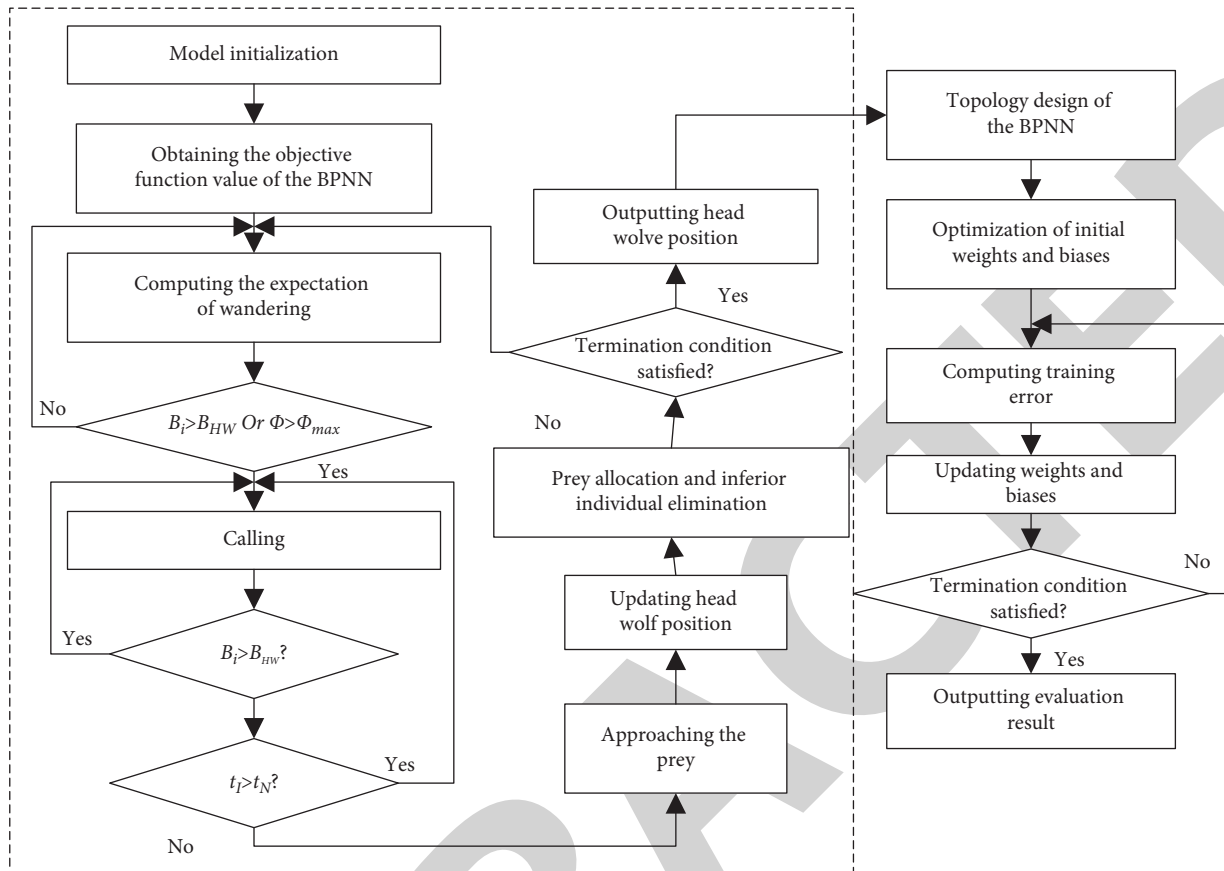


FIGURE 4: Flow of the late-phase online finance credit risk rating model.

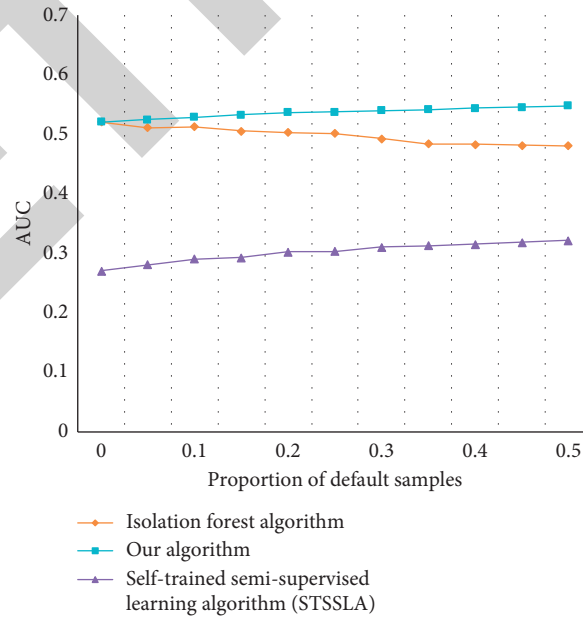


FIGURE 5: Influence of the proportion of potential default samples in labeled samples on the AUC. Note: AUC is short for area under the curve.

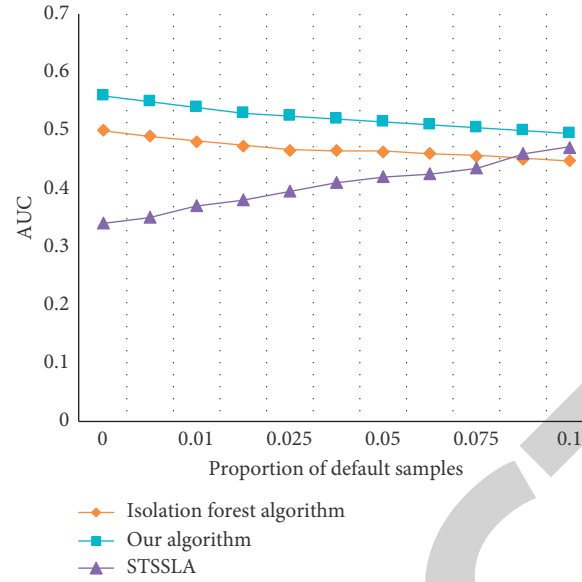


FIGURE 6: Influence of the proportion of potential default samples in unlabeled samples on the AUC.

TABLE 1: Prediction errors and time consumptions of different models.

| Serial number | Model | MSE | MTC | Serial number | Model | MSE | MTC |
|---------------|-----------|-------------------------|---------|---------------|-----------|-------------------------|---------|
| 1 | BPNN | 4.8763×10^{-2} | 19.7854 | 2 | BPNN | 5.1812×10^{-3} | 20.8921 |
| | GA-BPNN | 3.4221×10^{-2} | 14.1387 | | GA-BPNN | 4.1974×10^{-6} | 21.4613 |
| | Our model | 3.1986×10^{-7} | 11.9341 | | Our model | 8.3761×10^{-7} | 30.4897 |
| 3 | BPNN | 2.5405×10^{-5} | 22.7932 | 4 | BPNN | 3.2439×10^{-7} | 21.6495 |
| | GA-BPNN | 3.8873×10^{-6} | 18.9246 | | GA-BPNN | 5.7946×10^{-5} | 22.2056 |
| | Our model | 6.9249×10^{-8} | 12.1624 | | Our model | 9.3632×10^{-7} | 22.1632 |
| 5 | BPNN | 4.2126×10^{-4} | 21.7843 | 6 | BPNN | 2.0643×10^{-2} | 28.1989 |
| | GA-BPNN | 4.1934×10^{-6} | 20.6415 | | GA-BPNN | 6.3786×10^{-3} | 28.3894 |
| | Our model | 9.1507×10^{-7} | 16.7964 | | Our model | 8.3894×10^{-7} | 27.4891 |

Suppose there are 20 labeled samples in the early phase after the launch of an online finance credit product, including 10 normal samples and 10 potential default samples. Then, the proportion of potential default samples in unlabeled samples and test samples was adjusted from 0 to 0.1. Figure 6 shows the influence of that proportion on the AUC. With the growing proportion of potential default samples, the AUC of STSSLA increased to a certain extent, while that of our algorithm and isolation forest algorithm declined.

To verify the effectiveness of the late-phase credit risk rating model for online finance credit products, this paper applies the traditional BPNN and fuzzy BPNN separately on our samples for 200 iterations and compares their search results with the solution obtained by our model. Table 1 compares the prediction errors and time consumptions of these models. The convergence accuracy and efficiency of each model were measured by mean squared error (MSE) and mean time consumption (MTC), respectively.

As shown in Table 1, our model achieved a lower MSE in a shorter MTC than the BPNN and GA-BPNN in rating the postphase online finance credit risk. This is because the

traditional BPNN randomly initializes weights and thresholds, which lowers efficiency and accuracy. Experimental results show that our model overcomes this defect of the traditional BPNN and effectively improves the prediction performance.

Figures 7–9 provide the output error curve of our model during the training on different samples, MSE curves of our model, and the scatterplot of predictions and expectations on different samples. It can be seen that our model can effectively rate the postphase online finance credit risk.

Figure 10 compares the ROCs of our model before and after optimization. This paper adjusts the ratio of the loss of mistaking normal clients as default clients to the loss of mistaking default clients as normal clients. As shown in Figure 10, our model performed stably at different ratios. The AUCs of the original model and the improved model stabilized at 0.7231 and 0.8277, respectively. The optimized model obviously has better prediction ability.

Table 2 presents the confusion matrix of sample verification with different misjudgment ratios. Table 3 presents the confusion matrix of time verification with different

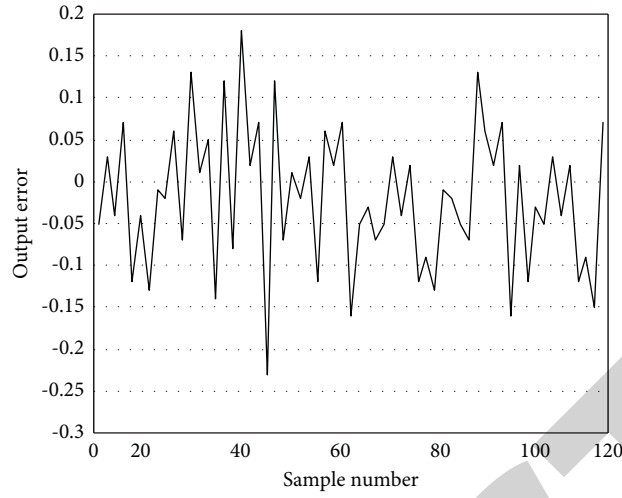


FIGURE 7: Output error curve on different samples.

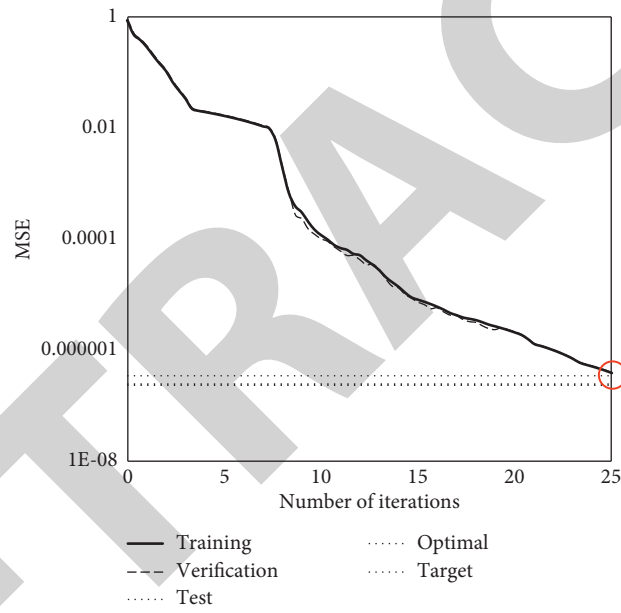


FIGURE 8: MSE curve of our model.

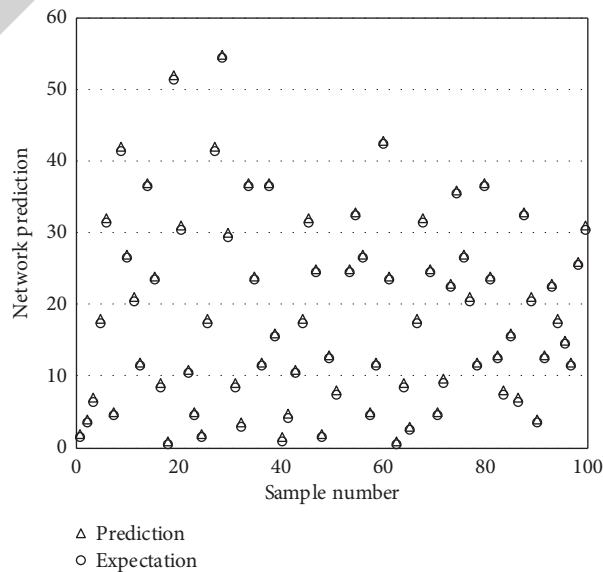


FIGURE 9: Scatterplot of predictions and expectations on different samples.

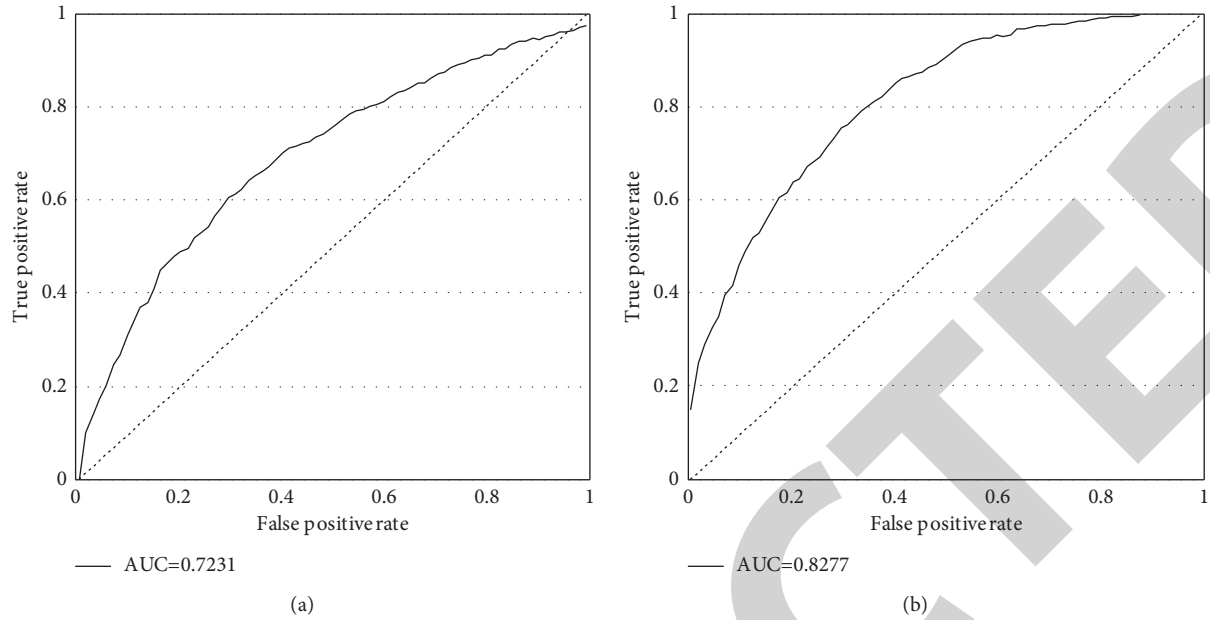


FIGURE 10: ROCs of the (a) original model and (b) improved model.

TABLE 2: Confusion matrix of sample verification with different misjudgment ratios.

| ν | 0.3 | | 0.5 | | 1.0 | | 2.0 | |
|------------------|-----|-------|-----|-------|-----|-------|-----|-------|
| Actual/predicted | 0 | 1 | 0 | 1 | 0 | 1 | 0 | 1 |
| 0 | 592 | 34 | 527 | 108 | 462 | 167 | 235 | 389 |
| 1 | 634 | 2,879 | 427 | 3,085 | 236 | 3,271 | 85 | 3,428 |

TABLE 3: Confusion matrix of time verification with different misjudgment ratios.

| ν | 0.3 | | 0.5 | | 1.0 | | 2.0 | |
|------------------|-----|-------|-----|-------|-----|-------|-----|-------|
| Actual/predicted | 0 | 1 | 0 | 1 | 0 | 1 | 0 | 1 |
| 0 | 96 | 3 | 97 | 5 | 81 | 19 | 32 | 66 |
| 1 | 156 | 1,915 | 67 | 2,001 | 27 | 2,042 | 11 | 2,057 |

misjudgment ratios. As expected, the number of normal clients being misjudged decreased with the growing loss, while the number of default clients being misjudged increased with the loss. Therefore, the confusion matrix outputted by our model changes with the demands of online finance credit businesses.

All in all, the above experimental results testify the superiority of our model in sample recognition accuracy, operating stability, and prediction power.

5. Conclusions

This paper explores the online finance credit risk rating based on the neural network. Specifically, the research period was divided into an early phase and a late phase by the launch of an online finance credit product. For the early phase, a cold start method was developed for the credit risk rating of online finance, and the similarity and abnormality

of credit default were calculated. For the late phase, the BPNN was improved to rate the online finance credit risk. Through experiments, the AUC curves were plotted with different proportions of potential default clients in labeled and unlabeled samples, and the prediction errors and time consumptions were compared between the BPNN, GA-BPNN, and our model. The results show that our model can effectively rate the postphase credit risk of online finance.

Data Availability

The data used to support the findings of this study are available from the corresponding author upon request.

Conflicts of Interest

The authors declare that they have no conflicts of interest regarding the publication of this paper.

References

- [1] X. Wanqin Yang and W. Yang, "Prediction and analysis of literature loan circulation in university libraries based on RBF neural network optimized model," *Automatic Control and Computer Sciences*, vol. 54, no. 2, pp. 139–146, 2020.
- [2] X. Zhu, "Deep learning modelling of systemic financial risk," *Revue d'Intelligence Artificielle*, vol. 34, no. 2, pp. 137–141, 2020.

- [3] A. Nagurney, "Networks in economics and finance in networks and beyond: a half century retrospective," *Networks*, vol. 77, no. 1, pp. 50–65, 2021.
- [4] R. Dekkers, R. de Boer, L. M. Gelsomino et al., "Evaluating theoretical conceptualisations for supply chain and finance integration: a Scottish focus group," *International Journal of Production Economics*, vol. 220, p. 107451, 2020.
- [5] F. Liu and Y. You, "A big data-based anti-fraud model for internet finance," *Revue d'Intelligence Artificielle*, vol. 34, no. 4, pp. 501–506, 2020.
- [6] J. Lopez-Jimenez, J. L. Gutierrez-Rivas, E. Marin-Lopez, M. Rodriguez-Alvarez, and J. Diaz, "Time as a service based on white rabbit for finance applications," *IEEE Communications Magazine*, vol. 58, no. 4, pp. 60–66, 2020.
- [7] L. A. Sauls, "Becoming fundable? Converting climate justice claims into climate finance in Mesoamerica's forests," *Climatic Change*, vol. 161, no. 2, pp. 307–325, 2020.
- [8] R. Chandra and S. Chand, "Evaluation of co-evolutionary neural network architectures for time series prediction with mobile application in finance," *Applied Soft Computing*, vol. 49, pp. 462–473, 2016.
- [9] H. Ghoddsi, G. G. Creamer, and N. Rafizadeh, "Machine learning in energy economics and finance: a review," *Energy Economics*, vol. 81, pp. 709–727, 2019.
- [10] A. Smolyak, O. Levy, L. Shekhtman, and S. Havlin, "Interdependent networks in economics and finance—a physics approach," *Physica A: Statistical Mechanics and Its Applications*, vol. 512, pp. 612–619, 2018.
- [11] M. Karimi and H. Saberi Nik, "A piecewise spectral method for solving the chaotic control problems of hyperchaotic finance system," *International Journal of Numerical Modelling: Electronic Networks, Devices and Fields*, vol. 31, no. 3, Article ID e2284, 2018.
- [12] A. Sanford and I. Moosa, "Operational risk modelling and organizational learning in structured finance operations: a Bayesian network approach," *Journal of the Operational Research Society*, vol. 66, no. 1, pp. 86–115, 2015.
- [13] A. Taufik and N. I. Soesilo, "The impact of loan to value to property credit growth sustainability in Indonesia," *IOP Conference Series: Earth and Environmental Science*, vol. 716, no. 1, Article ID 012091, 2021.
- [14] L. Han, L. Han, and H. Zhao, "Study and application of credit scoring models to appraisal of the loan to Chinese companies with uncertain linguistic information," *International Journal of Applied Cryptography: International Journal of Advancements in Computing Technology*, vol. 4, no. 6, pp. 43–49, 2012.
- [15] S. Purohit and A. Kulkarni, "Credit evaluation model of loan proposals for Indian Banks," in *Proceedings of the 2011 World Congress on Information and Communication Technologies*, pp. 868–873, Mumbai, India, December 2011.
- [16] U. R. Kamboh, Q. Yang, M. Qin, and S. Rauf, "Uncertainty cost analysis of heterogeneous wireless network based on loan repayment approach," in *Proceedings of the 2017 9th International Conference on Advanced Infocomm Technology (ICAIT)*, pp. 170–175, Chengdu, China, November 2017.
- [17] S. Chakraborty, J. Gaeta, K. Dutta, and D. Berndt, "An analysis of stability of inter-bank loan network: a simulated network approach," in *Proceedings of the 50th Hawaii International Conference on System Sciences*, Hilton Waikoloa Village, HI, USA, January 2017.
- [18] G. Bhat, S. G. Ryan, and D. Vyas, "The implications of credit risk modeling for banks' loan loss provisions and loan-origination procyclicality," *Management Science*, vol. 65, no. 5, pp. 2116–2141, 2019.
- [19] M. Leow and J. Crook, "Intensity models and transition probabilities for credit card loan delinquencies," *European Journal of Operational Research*, vol. 236, no. 2, pp. 685–694, 2014.
- [20] K. Choi, G. Kim, and Y. Suh, "Classification model for detecting and managing credit loan fraud based on individual-level utility concept," *ACM SIGMIS-Data Base: The DATABASE for Advances in Information Systems*, vol. 44, no. 3, pp. 49–67, 2013.
- [21] A. Sokolov, R. Webster, A. Melatos, and T. Kieu, "Loan and nonloan flows in the Australian interbank network," *Physica A: Statistical Mechanics and Its Applications*, vol. 391, no. 9, pp. 2867–2882, 2012.
- [22] Z. Xu, X. Cheng, K. Wang, and S. Yang, "Analysis of the environmental trend of network finance and its influence on traditional commercial banks," *Journal of Computational and Applied Mathematics*, vol. 379, Article ID 112907, 2020.
- [23] M. R. Fayyaz, M. R. Rasouli, and B. Amiri, "A data-driven and network-aware approach for credit risk prediction in supply chain finance," *Industrial Management & Data Systems*, vol. 121, no. 4, pp. 785–808, 2020.
- [24] A. Leng, G. Xing, and W. Fan, "Credit risk transfer in SME loan guarantee networks," *Journal of Systems Science and Complexity*, vol. 30, no. 5, pp. 1084–1096, 2017.
- [25] J. Juma and D. Gichoya, "Artificial neural network based expert system for loan application evaluation: case of Kenya commercial bank," in *Proceedings of the 2013 IST-Africa Conference & Exhibition*, pp. 1–11, Nairobi, Kenya, May 2013.
- [26] D. Maček, I. Magdalenić, and N. B. Ređep, "A systematic literature review on the application of multicriteria decision making methods for information security risk assessment," *International Journal of Safety and Security Engineering*, vol. 10, no. 2, pp. 161–174, 2020.
- [27] P. Wetzel and E. Hofmann, "Supply chain finance, financial constraints and corporate performance: an explorative network analysis and future research agenda," *International Journal of Production Economics*, vol. 216, pp. 364–383, 2019.
- [28] P. R. Srivastava, Z. J. Zhang, and P. Eachempati, "Deep neural network and time series approach for finance systems: predicting the movement of the Indian stock market," *Journal of Organizational and End User Computing*, vol. 33, no. 5, pp. 204–226, 2021.